NASA/TM-2006-213681

Aft-End Flow of a Large-Scale Lifting Body During Free-Flight Tests

Daniel W. Banks and David F. Fisher
NASA Dryden Flight Research Center
Edwards, California

June 2006

NASA STI Program ... in Profile

Since its founding, NASA has been dedicated to the advancement of aeronautics and space science. The NASA scientific and technical information (STI) program plays a key part in helping NASA maintain this important role.

The NASA STI program is operated under the auspices of the Agency Chief Information Officer. It collects, organizes, provides for archiving, and disseminates NASA's STI. The NASA STI program provides access to the NASA Aeronautics and Space Database and its public interface, the NASA Technical Report Server, thus providing one of the largest collections of aeronautical and space science STI in the world. Results are published in both non-NASA channels and by NASA in the NASA STI Report Series, which includes the following report types:

- TECHNICAL PUBLICATION. Reports of completed research or a major significant phase of research that present the results of NASA programs and include extensive data or theoretical analysis. Includes compilations of significant scientific and technical data and information deemed to be of continuing reference value. NASA counterpart of peer-reviewed formal professional papers but has less stringent limitations on manuscript length and extent of graphic presentations.

- TECHNICAL MEMORANDUM. Scientific and technical findings that are preliminary or of specialized interest, e.g., quick release reports, working papers, and bibliographies that contain minimal annotation. Does not contain extensive analysis.

- CONTRACTOR REPORT. Scientific and technical findings by NASA-sponsored contractors and grantees.

- CONFERENCE PUBLICATION. Collected papers from scientific and technical conferences, symposia, seminars, or other meetings sponsored or cosponsored by NASA.

- SPECIAL PUBLICATION. Scientific, technical, or historical information from NASA programs, projects, and missions, often concerned with subjects having substantial public interest.

- TECHNICAL TRANSLATION. English-language translations of foreign scientific and technical material pertinent to NASA's mission.

Specialized services also include creating custom thesauri, building customized databases, and organizing and publishing research results.

For more information about the NASA STI program, see the following:

Access the NASA STI program home page at http://www.sti.nasa.gov.

- E-mail your question via the Internet to help@sti.nasa.gov.

- Fax your question to the NASA STI Help Desk at (301) 621-0134.

- Phone the NASA STI Help Desk at (301) 621-0390.

- Write to:
  NASA STI Help Desk
  NASA Center for AeroSpace Information
  7121 Standard Drive
  Hanover, MD 21076-1320

NASA/TM-2006-213681

Aft-End Flow of a Large-Scale Lifting Body During Free-Flight Tests

Daniel W. Banks and David F. Fisher
NASA Dryden Flight Research Center
Edwards, California

National Aeronautics and
Space Administration

Dryden Flight Research Center
Edwards, California 93523-0273

June 2006

Available from the following:

NASA Center for AeroSpace Information
7121 Standard Drive
Hanover, MD 21076-1320
(301) 621-0390

National Technical Information Service
5285 Port Royal Road
Springfield, VA 22161-2171
(703) 605-6000

ABSTRACT

Free-flight tests of a large-scale lifting-body configuration, the X-38 aircraft, were conducted using tufts to characterize the flow on the aft end, specifically in the inboard region of the vertical fins. Pressure data was collected on the fins and base. Flow direction and movement were correlated with surface pressure and flight condition. The X-38 was conceived to be a rescue vehicle for the International Space Station. The vehicle shape was derived from the U.S. Air Force X-24 lifting body. Free-flight tests of the X-38 configuration were conducted at the NASA Dryden Flight Research Center at Edwards Air Force Base, California from 1997 to 2001.

NOMENCLATURE

C_D	drag coefficient
$C_{D,base}$	base drag coefficient
$C_{l,fin}$	fin rolling-moment coefficient
$C_{n,base}$	base yawing-moment coefficient
$C_{n,fin}$	fin yawing-moment coefficient
C_p	surface pressure coefficient
C_{l_o}	zero sideslip rolling-moment coefficient
C_{n_o}	zero sideslip yawing-moment coefficient
t	time, sec
TP1	test point 1
TP2	test point 2
x	axial distance, in
y	lateral distance, in
y/y*	ratio of perpendicular distance from leading edge to primary vortex separation line
z	vertical distance, in
α	angle of attack, deg
β	angle of sideslip, deg
δ	deflection angle, deg
Φ	roll angle, deg

INTRODUCTION

Many large-scale lifting body configurations have been flight tested over the past several decades. The majority were tested by NASA and the U.S. Air Force at Edwards Air Force Base, California. Several notable examples include the M2-F3 (Northrop Aircraft, Huntington Beach, California), the X-24A (Martin Aircraft Company, Baltimore, Maryland), and the HL-10 (Northrop Aircraft, Huntington Beach, California) lifting bodies (refs. 1–4) as shown in figure 1. Some of these configurations have displayed unusual behavior, such as poor lateral-directional stability and control, attributed largely to the aft end flow. Specifically, the flow on and between the vertical fins and its interaction with the base flow accounted for most of these unwanted characteristics. These configurations were modified to include a center fin on the M2-F2 (became M2-F3) and a leading-edge droop on the outer fins of the HL-10 to eliminate the unwanted behaviors.

More recently (ending in 2001), large-scale free-flight tests of the X-38 vehicle were conducted at Edwards AFB by the NASA Johnson Space Center (JSC) and Dryden Flight Research Center (DFRC). The outer mold line of the X-38 was derived largely from the X-24A lifting body shape. The test article, designated V131R (Scaled Composites, Mojave, California), is an 80-percent scale uninhabited vehicle with control inputs preprogrammed prior to separation from a B-52B (The Boeing Company, Chicago, Illinois) airplane in flight. The preprogrammed control inputs included maneuvers to determine vehicle behavior in addition to basic aircraft control. It is then recovered with a 5,500 ft^2 steerable parafoil.

Design and testing of the X-38 vehicle was lead by JSC with contributions from several other NASA Centers, the European Space Agency, and many other United States and European companies (ref. 5). As seen in figure 2, a DFRC B-52B airplane was used to drop the large-scale free-flight test vehicle over the test range. These flights revealed undesirable rolling and yawing characteristics, demonstrated by an uncommanded roll occurring during the first flight of V131R. During subsequent flights, it was desirable to characterize the flow on the aft end of the vehicle to determine the cause of this behavior. Ultimately, tufts on the inboard side of the fins were implemented and revealed a significant amount of information about the flow in this critical area. In addition, sensors were placed on the fins and base to measure the static pressures. The flow direction, movement, and differences from side to side were correlated with the pressure data and flight condition. Tufts are one of the most simple flow visualization techniques, yet can be useful in relatively harsh environments and complex tests.

EC69-2353

Figure 1. The X-24A, M2-F3, and HL-10 lifting bodies at the NASA Dryden Flight Research Center.

EC01-0339-33

Figure 2. The X-38 at release from the B-52B bomber.

EXPERIMENTAL APPROACH

Large-scale flight tests have been essential to determining the aerodynamic characteristics of lifting bodies at high Reynolds numbers. The X-38 was the latest lifting body program to undergo large-scale free-flight test.

X-38 Drop Test Series

The X-38 test program included a series of large-scale free-flight tests with test vehicles of increasing complexity. The final series of free-flight tests were conducted with V131R, which essentially replicated the outer mold line and all the control surfaces of the proposed flight vehicle. Figure 3 shows a three-view of the X-38 vehicle and figure 4 shows the X-38 (V131R) vehicle in flight. Anomalies observed in the past, primarily poor lateral-directional stability, had been attributed to aft end flow, specifically flow around and between the fins and the base, and interactions between the two. Prior to the second flight of V131R, these areas were instrumented to obtain data to clarify the specific flow characteristics with this vehicle. The instrumentation included tufting the inboard fin surfaces and measuring surface static pressures on the inboard fins and base. Between flights 2 and 3, additional tufts were added on the fins and pressure locations were moved to better define the flow field based on data obtained during flight 2.

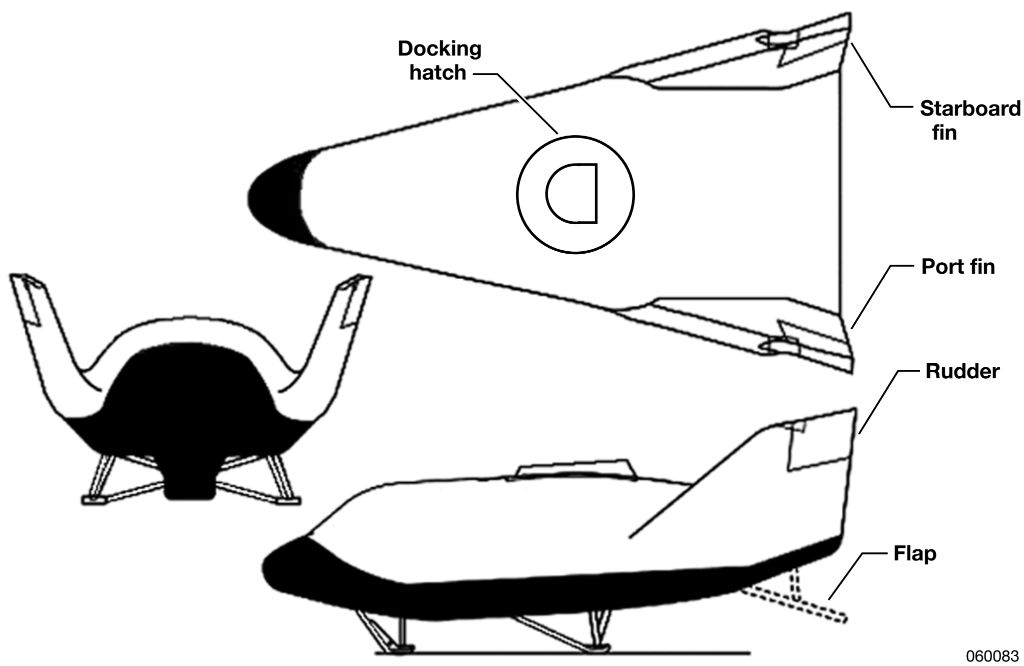

Figure 3. Three-view drawing of the X-38 vehicle.

EC01-0204-3

Figure 4. The X-38 in flight.

Tufting and Camera System

The tufts were arranged in a layout that avoided the pressure port orifices and still allowed for sufficient density and key locations to define the flow field. Shuttered video cameras (one for each fin) were placed in the area of the docking hatch cover to record the tuft motions during flight. The shutter speed was set to stop the movement of the tufts during each video frame. In addition to the video and still frames extracted from the video, techniques were used to clarify the differences between the port and starboard flows. As shown in figure 5, accurately measured benchmarks allowed for some quantitative tuft displacement to be measured and also allowed for the overlay of the fin images from the starboard and port sides, to determine the variation in flow between the two sides.

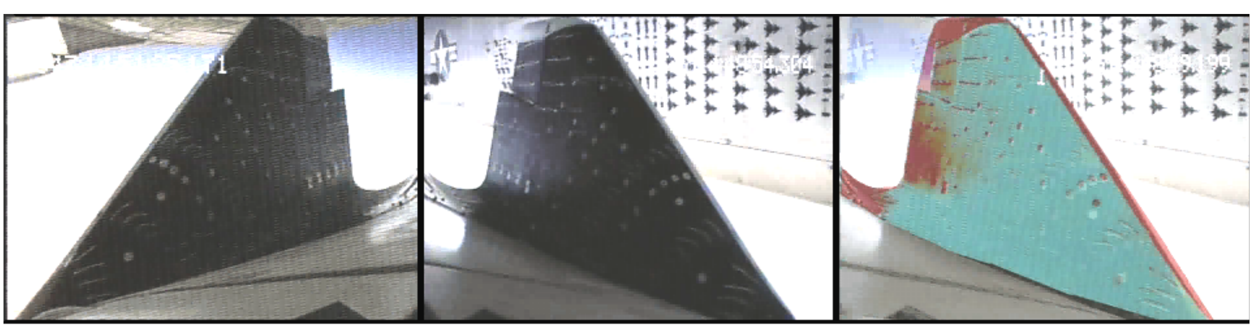

060084

Figure 5. Starboard, port, and overlay fin images prior to launch.

Fin Pressures

Fin surface pressures were measured during flight. A total of 25 pressures were measured on the inboard surface of each fin. The placements of these pressures were determined from wind tunnel and computational fluid dynamics (CFD) results for the expected flow field. In figure 6, an example of oil flow results from an earlier wind tunnel test of the X-38 aircraft is shown. The fin pressures were measured using electronically scanned pressure modules. These pressures were referenced to a holding tank, fed by an appropriately sized orifice, which was measured with an accurate absolute pressure transducer. Appropriately sized tubing (length and inside diameter) balanced the pneumatic lag of the fin and base orifices resulting from the rapidly changing ambient pressure (altitude decreasing rapidly results in ambient pressure increasing) (ref. 6).

The contribution of the fin aerodynamic loading to the overall yaw and rolling moments of the vehicle were calculated using weighted areas and comparing pressures on the left and right inboard fins. The locations of the pressure ports and reference areas are shown in figure 7. The fins are canted 16° to the vertical axis.

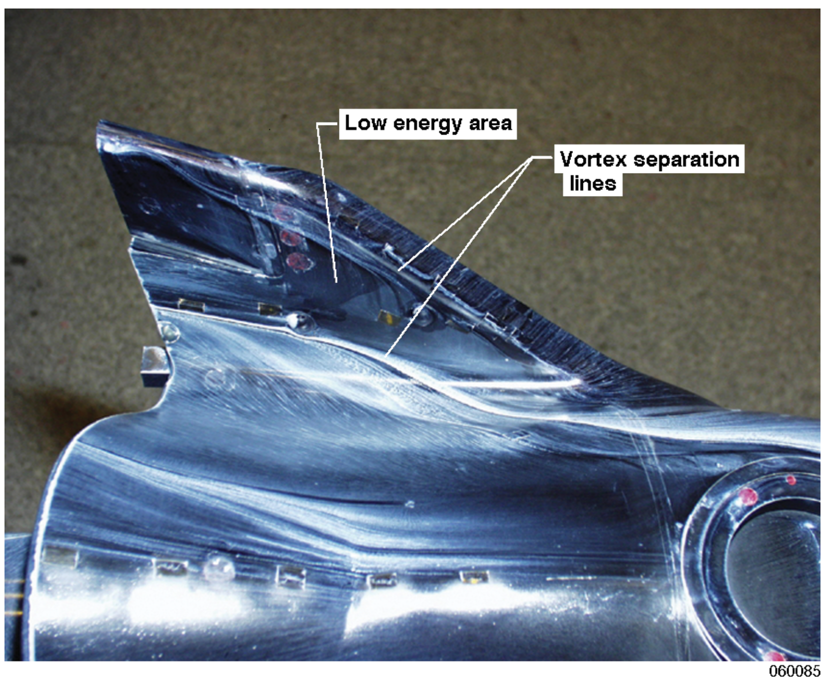

Figure 6. Example of wind tunnel oil flow over the port fin of an X-38 model.

#	Area	Orifice	ESP#
0+1	38.006	GX01P/GX01S	105/205
2	51.141	U0P/U0S	106/206
3	0	A5P/A5S	120/220
4a	**0**	**F1P/F1S**	**116/216**
4b	**10.8**	**A4P/A4S**	**117/217**
4c	**10.8**	**F2P/F2S**	**119/219**
4d	**10.8**	**F3P/F3S**	**121/221**
5	46.4	S1P/S1S	124/224
6	50.8	U2P/U2S	126/226
7	45.337	AA04P/GA04S	101/201
8a	**31.2**	**A3P/A3S**	**118/218**
8b	**50.8**	**F4P/F4S**	**122/222**
9	37.222	AS02P/GS02S	107/207
10	41.486	GX07P/GX07S	108/208
11	41.028	GA12P/GA12S	102/202
12	29.948	GX06P/GX06S	109/209
13	38.948	S3P/S3S	125/225
14	18.839	U3P/U3S	127/227
15	31.750	AA03P/GA03S	103/203
16	121.5	AS04P/GS04S	113/213
17	166.1	GX10P/GX10S	114/214
18	124.3	GX09P/GX09S	115/215

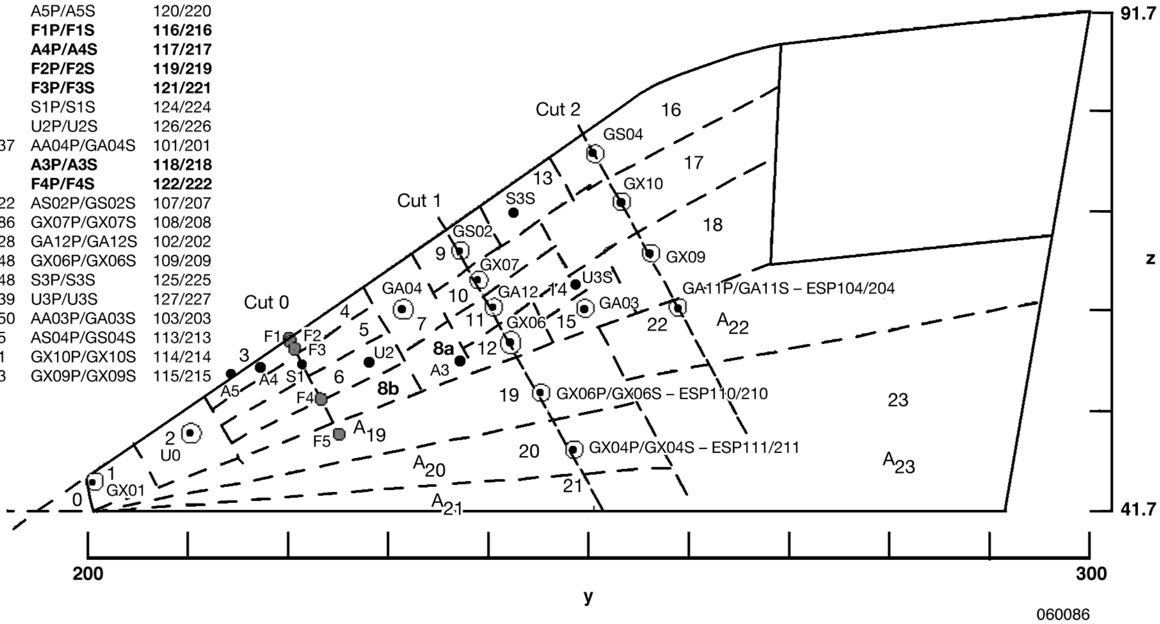

Figure 7. Fin orifice locations and load calculation areas.

Base Pressures

Base pressures were measured during flight to determine the contribution of the base to the yawing moment and to calculate base drag.

These pressures were measured with the same electronically scanned pressure units and reference tank as those on the fins. The number of pressures on the base was much lower than on the fins since high spatial resolution was not required on the base. The locations of the pressure ports and reference areas for the base are shown in figure 8. The data concerning the contribution of the base to overall vehicle yawing moment was desired, so the base was divided up into weighted areas and the pressures integrated to determine the contribution.

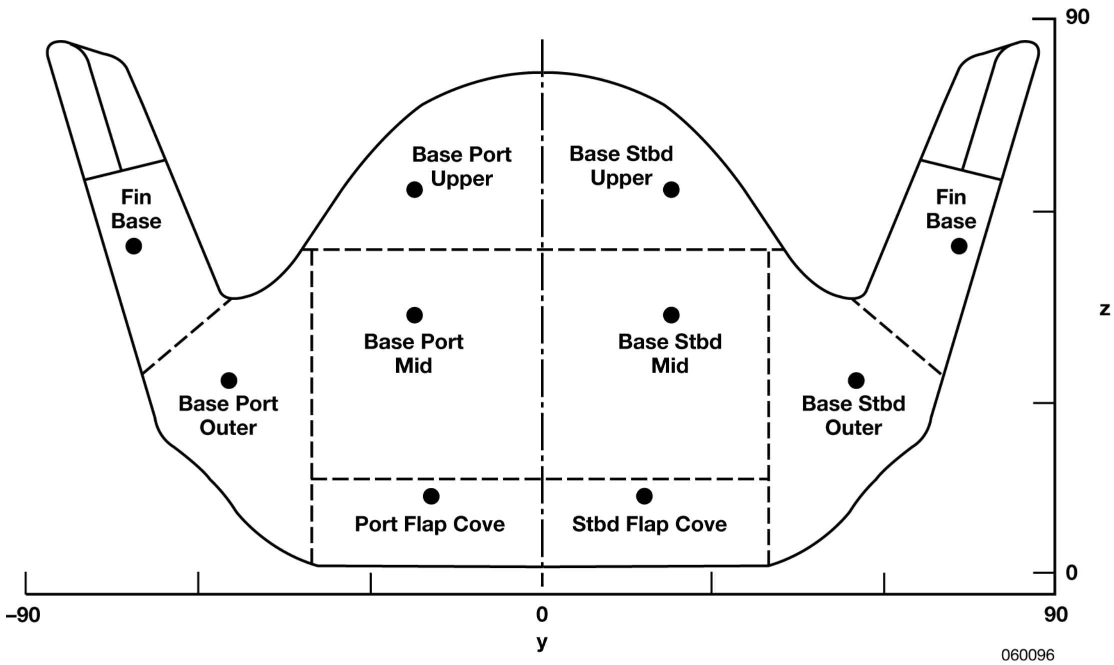

Figure 8. Base orifice locations and load calculation areas.

RESULTS AND DISCUSSION

The set of results from the third flight of the V131R free-flight tests is the most complete, and therefore is the basis of this report. Figure 9 shows the time history of the flight with regard to angle of attack (α), angle of sideslip (β), and rudder and flap position (δ). Two sets of flap doublets and rudder sweeps were performed to extract stability, control, and handling qualities data. There were two periods of time identified when the vehicle was stabilized, not performing large, preprogrammed control movements, and where β was close to zero. These two, short, quasi-stabilized periods of time will be used to determine the steady-state flow conditions and the component moment contributions. Test point 1 (TP1) is stabilized at $\alpha = 16°$ and test point 2 (TP2) at $\alpha = 18°$.

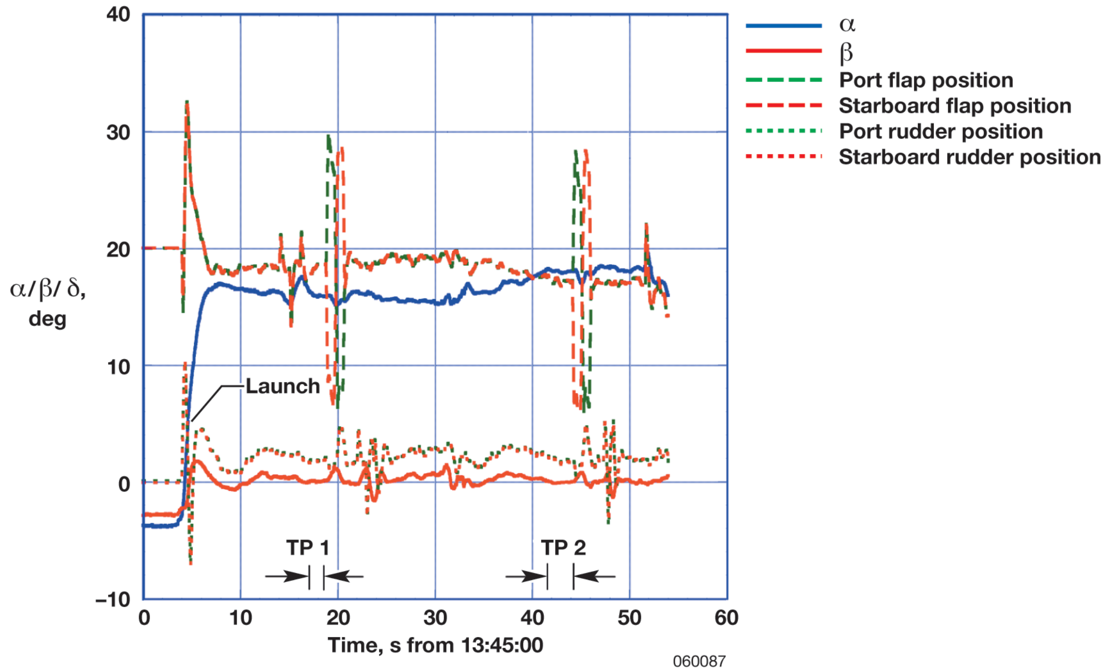

Figure 9. Flight conditions during flight 3 and test point periods.

General Flow Field of Lifting Body Configurations

The general flow field of a lifting body can be defined in terms of regions. The forebody region behaves much like that of an ogive forebody or similar object at angle of attack (refs. 7,8). Therefore, the incoming flow of the aft end likely has high angularity and some vorticity. The aft end flow consists of the fin flow, the body flow between the fins, the base flow, and flows in and around body flaps and control surfaces.

The fin flow behaves much like a highly swept lifting surface at high angles of attack. As such, the flow field is vortex dominated, with the vorticity initiated from the leading edge or near the leading edge. There are also significant areas of separated flow, recirculating regions, and dead zones. The rudder flows are very similar to an aft control surface on a highly swept lifting surface at high angles of attack.

The body flow between the fins is a transitioning zone from the body to the base and from the fins to the body. It is a highly interacting region and, like the fins, contains areas of vorticity, separated flow, recirculation, and dead zones. Unlike the fins, this region is not likely vortex dominated, despite the presence of some vorticity.

The base is an area of low-pressure and highly separated flow. The low pressure across the base is not necessarily uniform and can be a measurable contributor to the overall yawing moment of the vehicle, especially considering the large area of the base in this case. The overall base pressure appears bi-modal, favoring one side and then the other and can exhibit an oscillating

behavior, like a von Karman sheet (ref. 9). Obviously, the low pressure and large area means that the base is a large contributor to the vehicle drag. The flow behavior of the base is, to a large degree, influenced by the incoming flow from the body, fins, and body flaps. Conversely, the base flow likely affects the flow on the fins, especially in the root and base areas of the fins.

The body flaps are a very complex region because of the cavity flows, gap flows, and interactions between the two flaps. The flap cavities are likely a large recirculation area that favors one side depending on flap positions, vehicle orientation (such as sideslip angle), and possibly gap flow. This may be one cause of the bi-modal behavior of the base.

Tufts

The tufts provide a good overall visual picture of the highly complex flow field on and in the vicinity of the fins in dynamic flight conditions such as those experienced by the X-38 vehicle. Information can be obtained from the video, both in real time and slow motion, from still frames extracted from the video, and from enhanced video and frames. One enhancement method used was the overlay of one fin image on the other. Examples of this are shown in figures 10 and 11, for test points 1 and 2 respectively, on the far right. The white tufts are the starboard fin tufts and the red tufts are the port fin tufts. The overlay of images was very useful for determining flow differences between the two fins, especially during symmetric quasi-steady-state conditions. Please note that the starboard fin time code has approximately a two second bias. The other main enhancement technique was to extract and enlarge portions of images from frames at key times. Other techniques include changes to contrast, edge enhancements, frame averaging, and other common image processing methods.

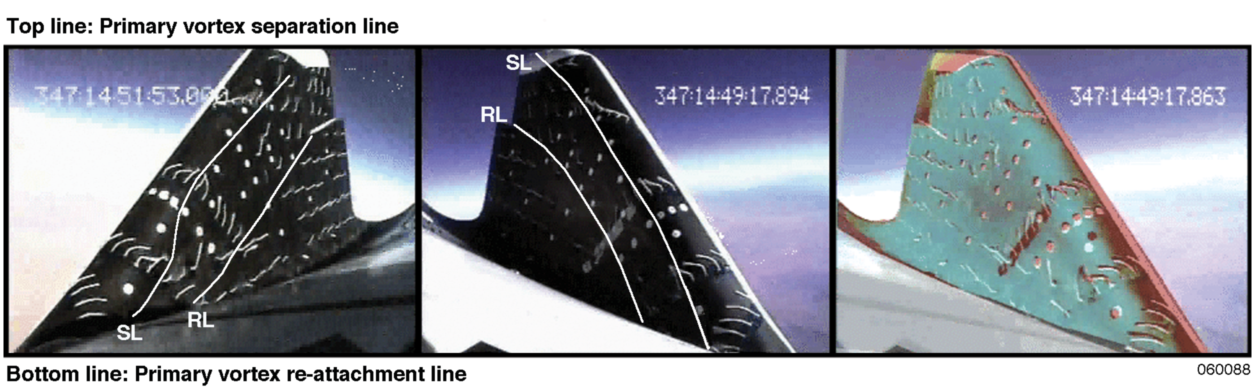

Figure 10. Starboard, port, and overlay fin images during test point 1.

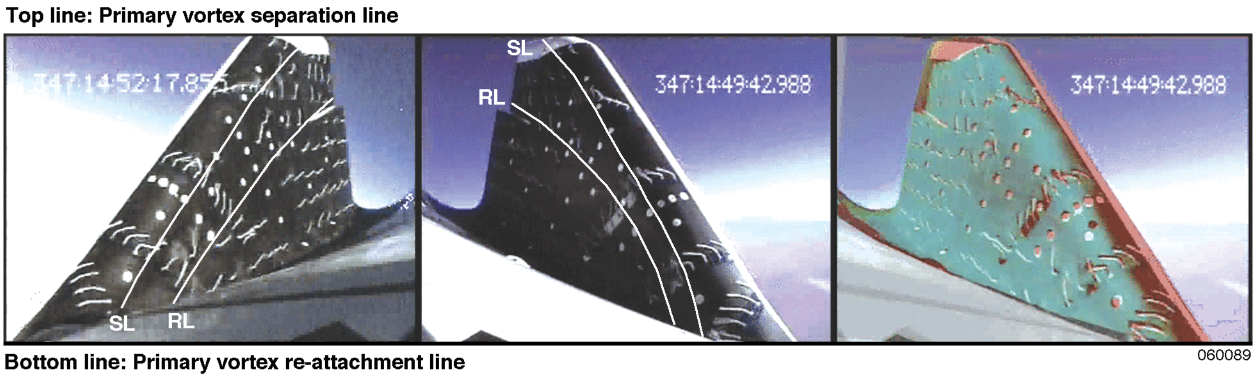

Figure 11. Starboard, port, and overlay fin images during test point 2.

Fin Pressures

The surface pressures complement the tuft data and provide quantitative data on the aerodynamic loads generated by the fins. The surface pressures for TP1 are shown in figure 12 and for TP2 in figure 13. Though the pressure data was not as extensive as previous comprehensive flight experiments, (refs. 10.11) the data is consistent with that in previous results. The suction peaks are the result of the higher local flow velocities while the lower suction pressures are present at the attachment and separation line. Though the tufts do not show any reversed flow, the pressure data suggests lower velocity flows near the fin root.

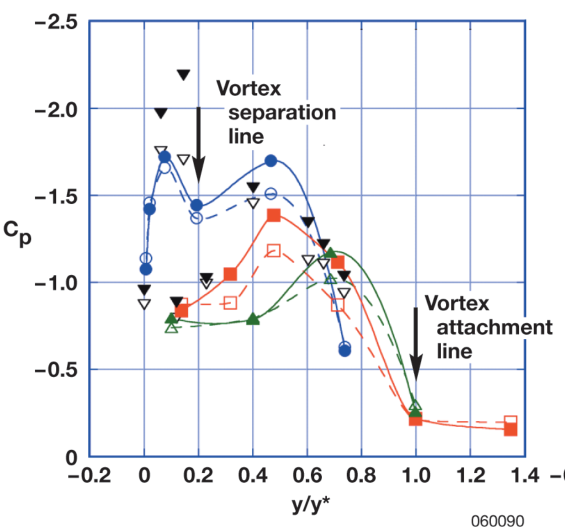

Figure 12. Fin pressure coefficients for test point 1.

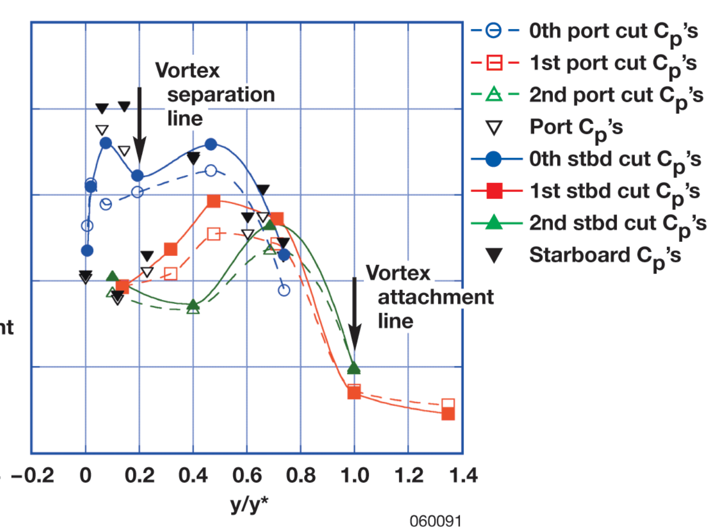

Figure 13. Fin pressure coefficients for test point 2.

A major challenge was determining the cause of a net yaw and roll bias of the vehicle. The fins were considered the most likely suspect followed by the base (including flap coves). Asymmetric flow between the port and starboard fins would be a probable cause of both the yaw and roll bias. The tuft data reveals subtle differences between the port and starboard fins. The pressure data also reveals significant differences between port and starboard pressure coefficients. Most noticeable are at the vortex suction peak near y/y* = 0.5 (cut 0 and cut 1) and 0.7 (cut 2). The data for both test points indicate the starboard fin is producing a higher net suction, and therefore lift, than that of the port fin. Enlarged views of the fin overlay, shown in figures 14 and 15, for TP1 and TP2 show that the starboard fin (white tufts) separation line is further toward the root than that of the port fin (red tufts). This implies that the area of attached accelerating flow, and therefore suction, is larger for the starboard fin. It is also consistent with a somewhat stronger primary vortex on the starboard fin, which would lead to increased overall suction. The tuft data indicates a potential mechanism of increased overall suction of the starboard fin.

Figure 14. Enlarged overlay near port U0 at test point 1.

Figure 15. Enlarged overlay near port U0 at test point 2.

Figure 16 shows the fin contribution to overall vehicle yawing moment (C_n) and rolling moment (C_1). The fins contribute a significant and predictable level of yaw and rolling moment based on vehicle sideslip angle, but the magnitude is not sufficient to account for the overall bias ($C_{n_o} \sim 0.004$; $C_{l_o} \sim -0.0015$). It was estimated that geometric airframe asymmetries accounted for approximately half of the C_n bias.

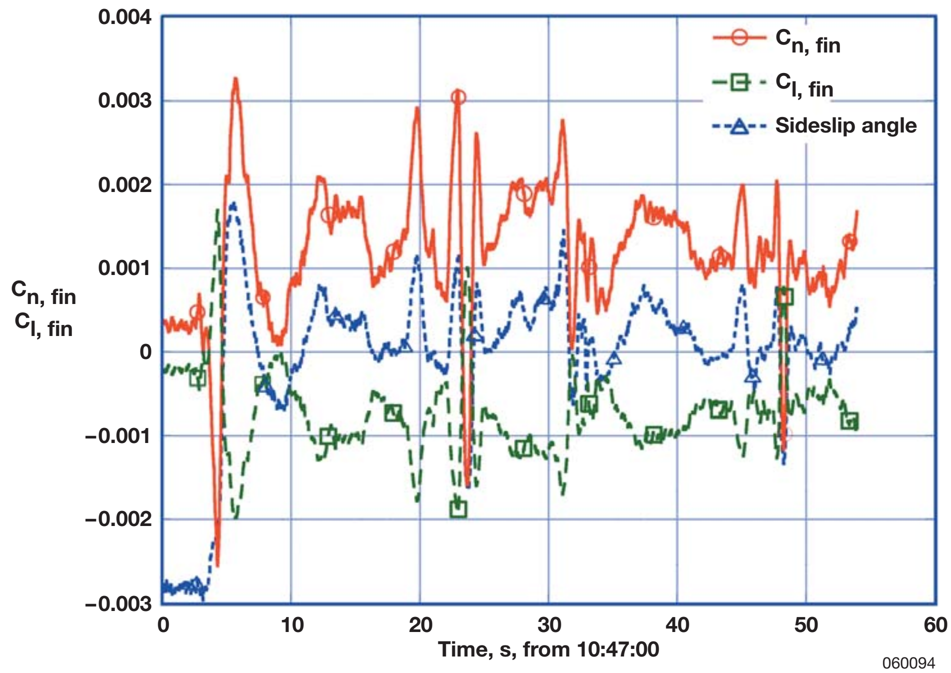

Figure 16. Fin induced rolling and yawing moment coefficients.

Base Pressures

The base pressures confirm a large region of low pressure, the center of which alternates from one side to the other, apparently being triggered by upstream flow or by the flap coves. The overall base fluctuates at approximately 1 Hz.

Static pressures in the base were used to calculate base driven yawing moments and base drag. The yawing moment contribution of the base, as shown in figure 17, is, at times, adding to the yawing moment of the fins and at other times, is reducing it. The base drag was calculated as approximately $C_{D,base} = 0.38$, significantly higher than previously tested lifting body configurations, and attributed to the large base area (ref. 4).

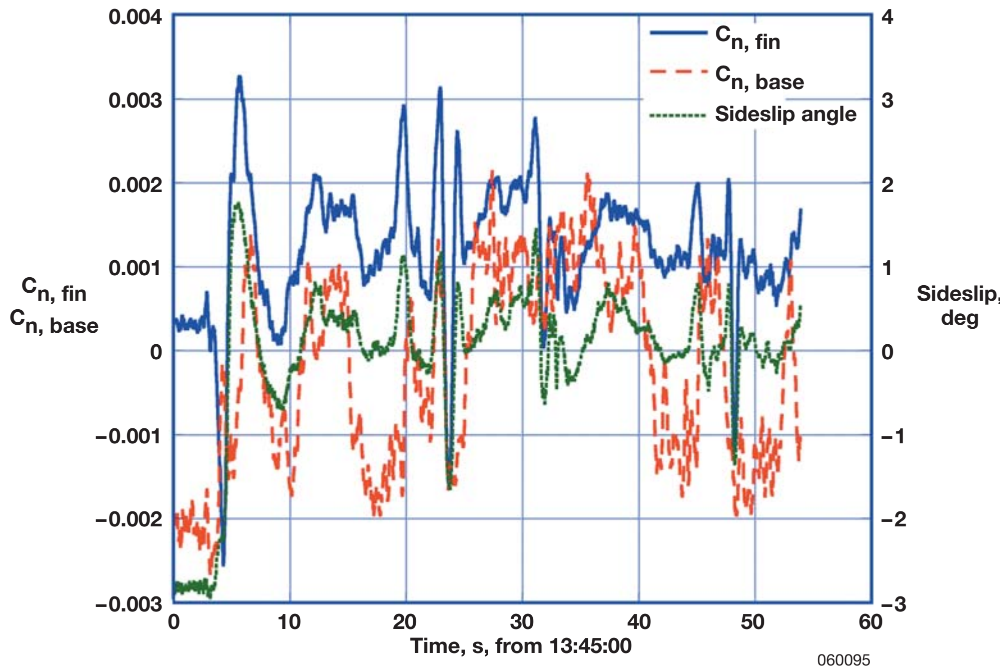

Figure 17. Base and fin induced yawing moment.

CONCLUDING REMARKS

A series of free-flight tests were conducted on a large-scale model of a proposed crew rescue vehicle, the X-38. These tests revealed some undesirable lateral-directional vehicle behavior reminiscent of that seen in early flight tests of large-scale lifting bodies. These behaviors were attributed largely to aft end flow. Testing continued after instrumenting the appropriate areas of the aft end of the test vehicle; including tufting the inboard surfaces of the fins, installing cameras to record the tufts, and installing surface pressure ports on the fins and base. The test results revealed a significant amount of information about the flow at the aft end of the vehicle. The results did not reveal a single cause ("smoking gun") for the undesirable behavior observed, but showed that it likely resulted from a complex interacting flow field. The fins are dominated by vortex flows with large suction peaks. The low pressure base has a bi-stable center of pressure that changes sides because of an inconclusive triggering mechanism and fluctuates at approximately 1 Hz.

Mechanical tufts combined with surface static pressures are a relatively simple and straightforward technique to diagnose a flow field, even in flight.

REFERENCES

1. Hallion, Richard P., *On the Frontier: Flight Research at Dryden*, *1946-1981*, NASA SP-4303, 1984.

2. Illiff, Kenneth W., and Curtis L. Peebles, *From Runway to Orbit: Reflections of a NASA Engineer,* NASA SP-2004-4109, 2004.

3. Reed, R. Dale, *Wingless Flight: The Lifting Body Story,* NASA SP-4220, 1997.

4. Saltzman, Edwin J., Charles K. Wang, and Kenneth W. Iliff, *Aerodynamic Assessment of Flight-Determined Subsonic Lift and Drag Characteristics of Seven Lifting-Body and Wing-Body Reentry Vehicle Configurations,* NASA/TP-2002-209032, November 2002.

5. Labbe, Steve G., Leo F. Perez, Steve Fitzgerald, Jose Longo, Marc Rapuc, and Rafael Molina, "X-38 NASA/DLR/ESA-DASSAULT Aviation Integrated Aerodynamic and Aerothermodynamic Activities," *Atmospheric Reentry Vehicles and Systems*, Arachon, France, March 1999.

6. Fisher, D., K.H. Horstmann, and H. Riedel, "Flight Test Measurement Techniques for Laminar Flow," *AGARDograph 300, Flight Test Techniques Series*, Vol. 23, Ch. 4.1, October 2003.

7. Hunt, B.L., "Asymmetric Vortex Forces and Wakes on Slender Bodies," AIAA 82-1336, *9th AIAA Atmospheric Flight Mechanics Conference*, San Diego, California, August 9–11, 1982.

8. Keener, Earl R., *Oil-flow separation patterns on an ogive forebody*, NASA/TM-81314, October 1981.

9. Komerath, N.M., R. Funk, R.G. Ames, R. Mahalingam, and C. Matos, *Low Speed Aerodynamics of the X-38 CRV: Summary of Research NAG9-927, 5/97-4/98*, NASA/CR-1998-208344, June 1998.

10. Peake, D.J., D.F. Fisher, and D.S. McRae, "Flight, wind tunnel, and numerical experiments with a slender cone at incidence," *AIAA Journal*, No. 10, October 1982, pp 1338–1345.

11. Fisher, David F., Daniel W. Banks, and David M. Richwine, *F-18 High Alpha Research Vehicle Surface Pressures: Initial In-Flight Results and Correlation with Flow Visualization and Wind-Tunnel Data*, NASA/TM-101724, August 1990.

12. Loe, Greg, Steve Munday, Jeremy Hart, and Scott Merkle, "X-38 Vehicle 131R Free Flights 1, 2 & 3: FCS & Aerodynamics Lessons Learned," AAS 02-073, *25th Annual AAS Guidance and Control Conference*, Breckenridge, Colorado, February 2002.

REPORT DOCUMENTATION PAGE	*Form Approved* *OMB No. 0704-0188*

1. REPORT DATE *(DD-MM-YYYY)*	**2. REPORT TYPE**	**3. DATES COVERED** *(From - To)*
30-06-2006	Technical Memorandum	

4. TITLE AND SUBTITLE
Aft-End Flow of a Large-Scale Lifting Body During Free-Flight Tests

5a. CONTRACT NUMBER

5b. GRANT NUMBER

5c. PROGRAM ELEMENT NUMBER

6. AUTHOR(S)
Banks, Daniel W.; Fisher, David F.

5d. PROJECT NUMBER

5e. TASK NUMBER

5f. WORK UNIT NUMBER
984754.02.07.02

7. PERFORMING ORGANIZATION NAME(S) AND ADDRESS(ES)
NASA Dryden Flight Research Center
P.O. Box 273
Edwards, California 93523-0273

8. PERFORMING ORGANIZATION REPORT NUMBER
H-2656

9. SPONSORING/MONITORING AGENCY NAME(S) AND ADDRESS(ES)
National Aeronautics and Space Administration
Washington, DC 20546-0001

10. SPONSORING/MONITOR'S ACRONYM(S)
NASA

11. SPONSORING/MONITORING REPORT NUMBER
NASA/TM-2006-213681

12. DISTRIBUTION/AVAILABILITY STATEMENT
Unclassified -- Unlimited
Subject Category 02 Availability: NASA CASI (301) 621-0390 Distribution: Standard

13. SUPPLEMENTARY NOTES
Banks, Dryden Flight Research Center; Fisher, Dryden Flight Research Center, retired
Prepared for the12th International Symposium on Flow Visualization, September 10-14, 2006, German Aerospace Center (DLR), Gottingen, Germany.

14. ABSTRACT
Free-flight tests of a large-scale lifting-body configuration, the X-38 aircraft, were conducted using tufts to characterize the flow on the aft end, specifically in the inboard region of the vertical fins. Pressure data was collected on the fins and base. Flow direction and movement were correlated with surface pressure and flight condition.The X-38 was conceived to be a rescue vehicle for the International Space Station. The vehicle shape was derived from the U.S. Air Force X-24 lifting body. Free-flight tests of the X-38 configuration were conducted at the NASA Dryden Flight Research Center at Edwards Air Force Base, California from 1997 to 2001.

15. SUBJECT TERMS
Free flight, Lifting body, Surface pressures, Tufts, X-38

16. SECURITY CLASSIFICATION OF:			**17. LIMITATION OF ABSTRACT**	**18. NUMBER OF PAGES**	**19a. NAME OF RESPONSIBLE PERSON**
a. REPORT	**b. ABSTRACT**	**c. THIS PAGE**			STI Help Desk (email: help@sti.nasa.gov)
					19b. TELEPHONE NUMBER ***(Include area code)***
U	U	U	UU	20	(301) 621-0390

Standard Form 298 (Rev. 8-98)
Prescribed by ANSI Std. Z39-18